RESEARCH PAPER

Highly efficient nitrobenzene photoreduction over the amino acid-modified CdS-TiO_2 nanostructures under visible light

Mohsen Padervand [1]*, Atefeh Rahmani [2], Sara Rahimnejad [3], Mohammad Reza Gholami [2]

[1] Faculty of Science, Department of Chemistry, University of Maragheh, Maragheh, Iran

[2] Department of Chemistry, Sharif University of Technology, Tehran, Iran

[3] Department of Chemistry, Islamic Azad University, Shahr-e-Rey Branch, Tehran, Iran

ARTICLE INFO

Article History:
Received 21 April 2017
Accepted 22 June 2017
Published 1 July 2017

Keywords:
Amino acid
CdS-TiO_2
Microemulsion-mediated solvothermal method
Nitrobenzene

ABSTRACT

CdS-coupled TiO_2 nanocrystals were prepared by the microemulsion-mediated solvothermal method at pretty low temperatures. The semiconductor nanocrystals were modified with tyrosine, phenyl alanine, glysine and glutamate aminoacids and then were characterized by BET, SEM, EDX, XRD, UV–Vis spectroscopy, and FTIR analysis methods. The specific surface area and the average pore diameter were found to be about 470 $m^2 g^{-1}$ and 2.8 nm, respectively. Moreover, the average size of the CdS-TiO_2 particles was evaluated to be 28 nm. The results showed that the modification process with the aminoacids improves the adsorption capability and photoactivity of the samples. Among them, tyrosine was determined to be the best choice. According to the results, modification of CdS-TiO_2 heterojunction photocatalyst with electron-donating groups is an efficient strategy to increase the photoreduction of nitroaromatic compounds. Reusability experiments were also carried out and confirmed the high capacity of the prepared samples for the photoconversion of nitrobenzene after being repeated for four times.

How to cite this article
Padervand M, Rahmani A, Rahimnejad S, Gholami MR. Highly efficient nitrobenzene photoreduction over the amino acid-modified CdS-TiO_2 nanostructures under visible light. Nanochem Res, 2017; 2(1):109-119. DOI: 10.22036/ncr.2017.01.010

INTRODUCTION

Nitrobenzene is considered to be a highly toxic aromatic compound which is widely used in explosives, pesticides, prepharmo, dye production, lubricating oils, refinement, soaps or shoe polish production and so on. As a suspected carcinogenic and toxic compound, it releases nitrobenzene to the environment and poses a high threat to the human health. It may carry a high risk for the environment, even at low concentrations [1]. The strong electron affinity of nitro reduces the electron cloud density of the benzene ring and makes nitrobenzene very stable. Therefore, nitrobenzene is listed as one of the prior pollutants by many countries. Conventional methods for the removal of nitrobenzene from aqueous solutions can be divided into three main categories: physical, chemical and biological treatments [2-5]. Mineralization of nitrobenzene by microorganisms is prevented by the electron-deficient character of the nitro-group. Due to electron-deficiency, oxidation of nitroaromatic compounds is very difficult to achieve [6]. Therefore, conventional biological treatment processes are not effective for the treatment of nitrobenzene-rich wastewater. Nanosized particles of titanium dioxide have remarkable photocatalytic properties and have many applications in medicine, construction and environmental remediation. Lots of efforts have been made to modify titania to enhance the photocatalytic performance and develop multifunctional materials. It has been reported that the composite structure can affect the catalytic activity of catalytic nanostructures [7-15].

CdS–TiO_2 is an excellent candidate for photodecomposition of pollutants as result of

* Corresponding Author Email: *mohsenpadervand@gmail.com, padervand@maragheh.ac.ir*

its intrinsic energy band gap. The main drawback of TiO_2 is its large band-gap (anatase: 3.2 eV and rutile: 3.0 eV). As a consequence, TiO_2 shows the photoactivity only in the near ultraviolet region and can harvest only a small fraction (<5%) of incident solar irradiation [16]. CdS is very unstable against the photocorrosion in aqueous solutions under irradiation unless the solutions contain sacrificial agents, such as S^{2-} and/or SO_3^{2-} [17, 18]. They can compensate the disadvantages of individual component and induce a synergistic effect such as an efficient charge separation and improve the photostability. CdS is a fascinating material having ideal band gap energy. Recently, the surface complexation of TiO_2 nanocrystals with some benzene derivatives [19], amino carboxylic acids [20, 21] and arginine [22] resulted in enhancement of reduction properties of photogenerated electrons [23, 24]. These works investigated the surface modification of CdS-TiO_2 composites with specific chelating agents that may enhance both redox properties and adsorption capability of nitroaromatic compounds in order to develop a useful strategy for photocatalytic removal of nitroaromatics from waste water.

The most important advantages of the microemulsion method are to provide a transparent, isotropic and thermodynamically stable synthesis medium. In particular, water-in-oil microemulsions are formed by well-defined nanodroplets of the aqueous phase, dispersed by the assembly of surfactant molecules in a continuous oil phase. These nanodroplets can provide a restricted reaction media to control the shape and size distribution of particles prepared by precipitating.

We used a microemulsion approach to facilitate the direct formation of nanocrystalline TiO_2 coupled with the CdS nanocrystals at a considerably lower temperature by the solvothermal method [25]. This method can prevent the oxidation of CdS in CdS/TiO_2 nanocomposite during thermal treatment for the crystallization of TiO_2 [26]. Afterward, the activities of the prepared samples were evaluated by selective photoreduction of nitrobenzene to aniline under visible light.

EXPERIMENTAL

Materials and methods

Titanium tetraisopropoxide (TTIP) was used as a titanium source. $Cd(NO_3)_2$ and $(NH_4)_2S$, which were used as CdS precursors, and nitrobenzene (NB) were purchased from Merck company (Germany). A typical synthesis of (CdS at 3%) involved the use of cyclohexane (0.9 mol) as oil phase, Triton X-100 (0.028 mol) as surfactant and 1-hexanol (0.056 mol) as cosurfactant [25]. Three microemulsions containing 1mL of water (A), 1.5 mL of 0.3M $Cd(NO_3)_2$ solution (B) and 2.5mL of 20 wt% $(NH_4)_2S$ solution (C) were prepared. Titanium isopropoxide (14.55 mmol) was added to microemulsion (A) under continuous stirring. After titanium isopropoxide was gradually hydrolyzed and condensed in water nanodroplets for 30 min, microemulsion B was mixed with microemulsion A under vigorous agitation and sonicated for 5 min. Microemulsion C was then added into the mixture and sonicated for 5 min. This new microemulsion was stirred for 24 h at room temperature. In this process, cadmium sulfide was incorporated into the TiO_2 colloids by simultaneous coprecipitation of $Cd(NO_3)_2$ and $(NH_4)_2S$ in the water nanodroplets. The resulted microemulsion containing CdS and TiO_2 particles was placed in a 100 mL Teflon-lined stainless steel autoclave which is initially bubbled with N_2 gas for 10 min and then solvothermally treated at 180 ˚C for 16 h.

The obtained yellow slurry was centrifuged and washed with ethanol and water before finally being kept in a desiccator for drying. The modified CdS-TiO_2 catalyst (0.5 g) was achieved by soaking the prepared CdS-TiO_2 in the amino acid ethanolic solution (50 mL, 0.01 M) and sonicating for 10 min in order to have a well dispersed and homogenous surface at room temperature. It was soaked for 24 h and then dried. Once amino acids were anchored to TiO_2 particles, they were strongly bounded to it [27].

Characterization

The residual concentration of NB at different times was measured on a GC (Agilent, 6890 series, USA) (60 m HP-5 column, film thickness 1 µl, inside diameter 0.25 mm and FI detector). The X-ray diffraction (XRD) pattern of prepared samples was recorded on Bruker D8 advance X-ray diffractometer with CuKα irradiation (λ= 0.15406). The FTIR spectra were performed on the NB series spectrometer. The specific surface area of photocatalysts was calculated from the N_2 adsorption-desorption isotherm at 77 K, using Belsorp apparatus. The average particle size and morphology of photocatalysts were distinguished by scanning electron microscope (SEM) (XL30 model). An OSRAM 125 W lamp was used as a visible source as we can see the emission spectra of the illumination source in Fig. 1. Diffuse reflectance spectroscopy (DRS) analysis was performed

with a UV spectrophotometer (GBC Cintra40). The specific surface area of photocatalysts was calculated from the N_2 adsorption-desorption isotherm at 77 K, using Belsorp apparatus.

Photocatalytic activity

The photocatalytic activity measurements for the degradation of NB were performed in a quartz reactor that was placed 10 cm in front of the visible lamp with 125 W and surrounded by a circulating water jacket (Pyrex) to cool the lamp. 0.1 g of the prepared photocatalyst was suspended in a 100 mL aqueous solution of 0.0136 M (NB) whose pH has been adjusted by phosphate buffers. Prior to irradiation, the suspensions were magnetically stirred in the dark for 10 min to ensure the establishment of an adsorption/desorption equilibrium among the photocatalyst. At given irradiation time intervals of 20 to 120 min, 2.5 ml of the suspensions was collected, then centrifuged and filtered to separate the photocatalyst particles.

The aqueous solutions obtained from filtration of the samples were extracted three times with CH_2Cl_2. The organic extracts were concentrated under a stream of nitrogen and analyzed by GC/MS (Agilent 6890) . The oven temperature was programmed as follows: isothermal at 40 °C for 3 min, from 40 °C to 260 °C at 10 °C/min, and isothermal at 260 °C for 1 min. The conversion of NB in the reaction process could be calculated by using the following formula [20]:

$$\% \text{ Conversion} = C_0 - C_n / C_0 \times 100$$

where C_n and C_0 are the measured and initial concentration of NB respectively.

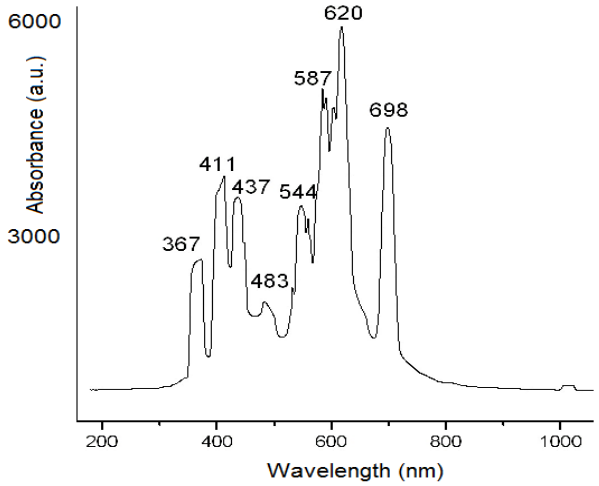

Fig. 1. The emmision spectra of 125 w mercury lamp

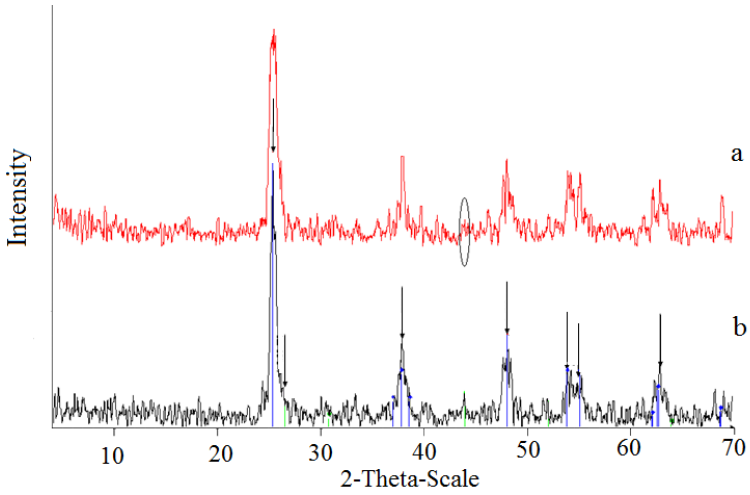

Fig. 2. XRD patterns of CdS-TiO_2-Tyrosine (a) after calcination (b) without calcinations.

RESULTS AND DISCUSSION

Characterization

XRD analysis

The XRD patterns of CdS-TiO_2-Tyrosine are represented in Fig. 2. Due to the low amount of loaded amino acid, the new diffraction peaks did not appear in the pattern of photocatalyst contained amino acid compared to pure CdS-TiO_2 sample. The results reveal that the peaks intensity of crystalline phases of samples has not changed before and after calcination, and it can be seen that there is no obvious difference. The results show that the crystalline phase of TiO_2 and CdS has not changed after the modification with Amino acid. The characteristic peaks in 2θ= 25.2˚, 37.92˚ and 48.02˚ correspond to the anatase TiO_2. The additional peaks at 26.5˚, 43.9˚, 52.1˚ which can be assigned to the CdS cubic phase (1 1 1), (2 0 0), (2 2 0) and (3 1 1) crystal planes, respectively, were also observed in Fig. 2 [25].

FTIR analysis

To understand the details of photocatalytic mechanism of the prepared composites, the FTIR analysis was conducted after the experiments while acidity conditions were changed. Fig. 3 shows the

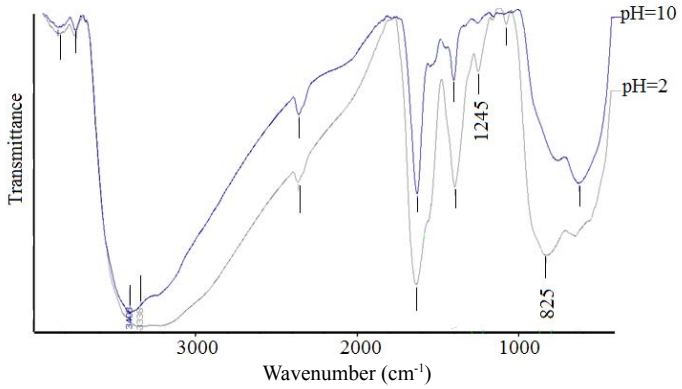

Fig. 3. FTIR spectra of CdS-TiO_2-Tyrosine after using in acidic and basic conditions

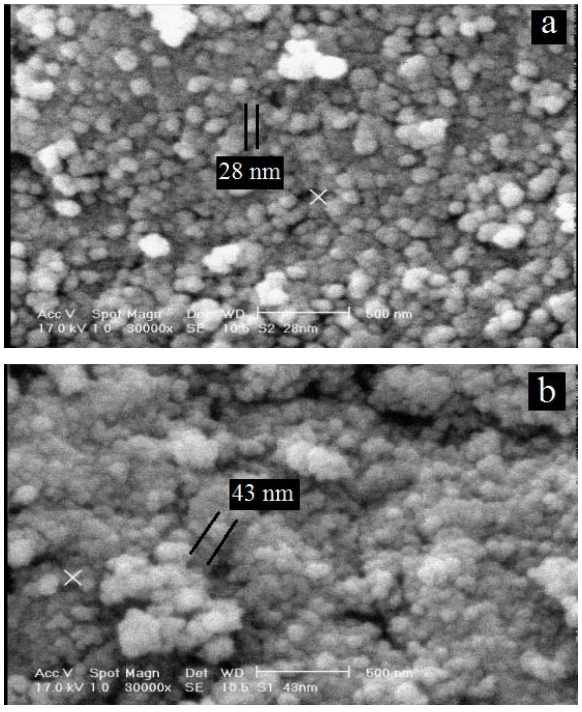

Fig. 4. SEM micrographs of samples (a: CdS-TiO_2 with the average particle size 28 nm, b: CdS-TiO2-Tyrosine with the average particle size 43 nm)

FTIR spectra of the extracted photocatalyst after being tested in acidic (a) and basic (b) conditions. The peak appearance in 825 cm^{-1} can be related to the N-H bond and also to the stretching C-N bond. Both peaks indicate that the compounds such as aniline can be adsorbed on the catalyst surface by donating groups and enhancing the photocatalytic activity. We suggest that aniline acts as a hole scavenger and that its presence on the surface decreases the electron-hole recombination and increases the photocatalytic efficiency. The peaks around 3400 cm^{-1} and 1600 cm^{-1} are due to O–H stretching and O–H bending modes, respectively. Also, the peaks related to Ti-O and Cd-S appear in the frequencies lower than 700 cm^{-1}.

SEM analysis

The SEM images of the prepared nanostructures are shown in Fig. 4. The micrographs show that the distribution of the surface particles is homogenous. The microemulsion synthesis method achieves the homogenous and average small particle size (28 nm), although the surfactant plays the role of controlling particle size and inhibiting the coagulation. Modifying CdS/TiO_2 nanocomposite with amino acid, the surface homogeneity has not changed, however the variation of the average particle size is observed.

The microemulsion method benefits droplet water as the microreactor which can provide the proper media for nucleation and controlling the

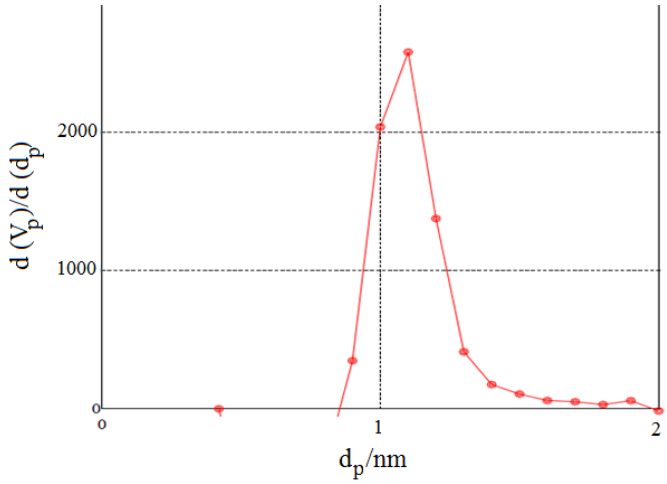

Fig. 5. MP-Plot pore size distributions of $CdS-TiO_2$

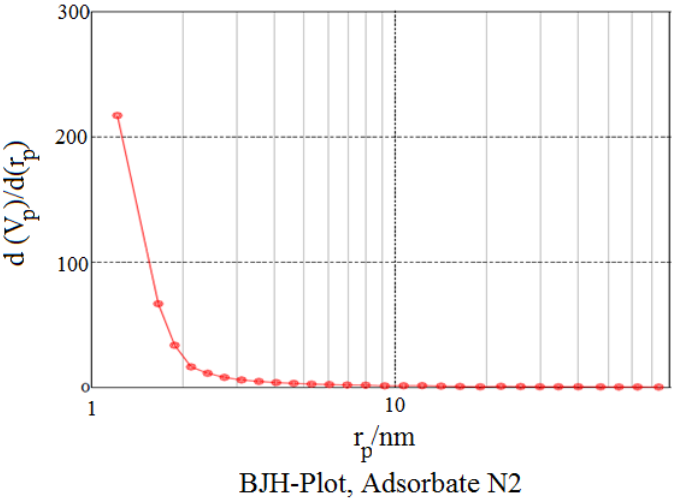

Fig. 6. BJH pore size distributions of $CdS-TiO_2$

Table 1. Summary of the physicochemical properties of the samples

Sample	S_{BET} [a] ($m^2 g^{-1}$)	Mean pore [b] size (nm)	Total pore [c] volume($cm^{-3} g^{-1}$)
CdS-TiO_2	423.94	2.8397	0.3010
CdS-TiO_2-Tyrosine	470.74	2.8655	0.3372

a BET surface area calculated from the linear part of the BET plot.
b Estimated using the BJH desorption branch of the isotherm.
c Single point total pore volume of pores at $P/P_0 = 0.97$.

growth process of the particles. In the process of modifying by amino acid, the organic solvent such as methanol was used. This organic solvent prevents the agglomeration of nanoparticles. As a result, the average particle size has been increased to 43 nm which is due to the presence of the organic layer (the aminoacids) covered the surface of CdS-TiO_2 nanoparticles. The SEM micrograph indicates that the bulk particles have a spherical shape before and after loading the amino acids and a porous structure could be observed in all samples.

BET analysis

Table 1 shows the surface area and pore size distribution of CdS-TiO_2, CdS-TiO_2-Tyrosine photocatalysts. The data demonstrated that modifying CdS-TiO_2 by amino acid increased the surface area but did not change the pore volume and the average pore diameter. On the basis of the hysteresis loop, adsorption and desorption branches of CdS-TiO_2 and CdS-TiO_2-Tyrosine have not changed. The results indicated that modifying with amino acid has not influenced the surface morphology. The MP-Plot (Fig. 5) and BJH (Fig. 6) of the CdS-TiO_2, CdS-TiO_2-Tyrosine show that the pore diameter was narrow, mainly below 2 nm. BJH plots are not a conventional Gussian curve, indicating the micropore size.

Table 2. Elemental Analysis of photocatalysts (CdS-TiO_2 and CdS-TiO_2-Tyrosine)

Sample	Element	W%	At%
CdS-TiO_2	S	3.93	5.84
	Cd	2.52	1.07
	Ti	93.55	93.09
CdS-TiO_2-Tyrosine	S	3.72	5.61
	Cd	4.64	2
	Ti	91.63	92.40

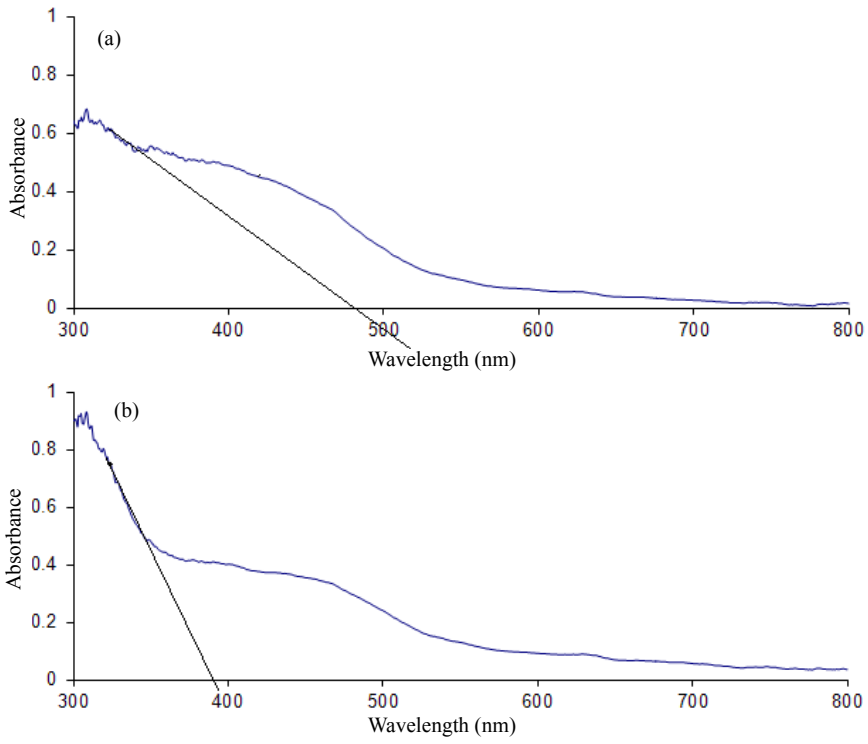

Fig. 7. UV–vis absorption spectra of prepared photocatalysts (a: CdS-TiO_2-Tyrosine, b: CdS-TiO_2)

Energy dispersive X-ray (EDX) analysis

The elemental contents of CdS-TiO_2 and CdS-TiO_2-Tyrosine composite listed in Table 2 show that Ti, O, Cd and S are mainly elemental contents of CdS-TiO_2 and catalyst purity. The amount of amino acid is so small that no related elemental contents are observed in the EDX analysis, which is consistent with the XRD patterns.

UV–Vis diffuse refection spectroscopy

The diffused reflectance UV–Vis absorption spectra of the CdS/TiO_2 and CdS-TiO_2-Tyrosine are shown in Fig. 7. The CdS/TiO_2 sample exhibits the strong absorption peaks in the visible region and the peaks related to CdS-TiO_2-Tyrosine shift to a longer wavelength. It shows that amino acid as an impurity induces a few levels between the valence and conduction band of the composite. In addition, the edges of the absorption of CdS-TiO_2-Tyrosine sample were shifted to approximately 472.1 nm, corresponding to band gap energy of 2.62 eV [14, 16]. The absorption onsets were determined by linear extrapolation from the inflection point of the curve to the baseline. To compare, the absorption onsets for CdS-TiO_2 and CdS-TiO_2-Tyrosine were determined 392.56 and 472.1 nm, corresponding to band gap energies of 3.16 and 2.62 eV, respectively.

Photoconversion of nitrobenzene (NB)

Effect of surface modification on the adsorption capability

It is obvious that in the heterogeneous photocatalysis the efficiency of photocatalytic reaction is affected by the surface adsorption of organic compounds. The adsorption capability of the modified CdS-TiO_2 photocatalysts as a different type of amino acids was investigated and a comparison with CdS/TiO_2 was made. The results showed that the adsorption capability greatly increased in all modified photocatalysts. The hydrogen bonding and the n-π and π-π interactions between the modified TiO_2 and nitrobenzene are responsible for the stronger adsorption capability [2]. The results for this study are shown in Fig. 8.

The effect of modification on the photoconversion efficiency

Fig. 8 shows the results for the conversion of nitrobenzene over different modified CdS-TiO_2 photocatalysts in the aqueous medium. From Fig. 9

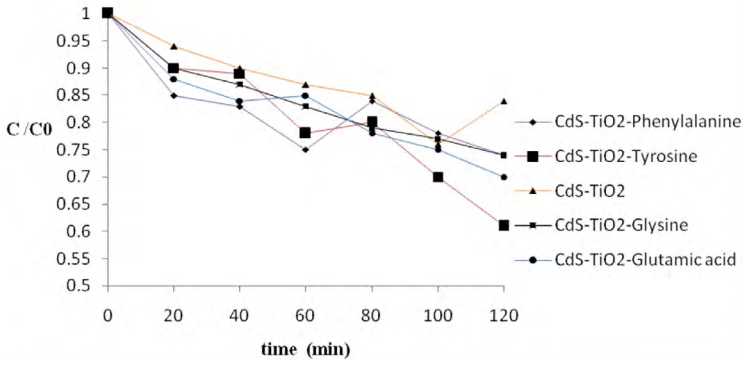

Fig. 8. Effect of surface modification on the adsorption capability (catalyst: 0.1 g, NB: 0.0136 M)

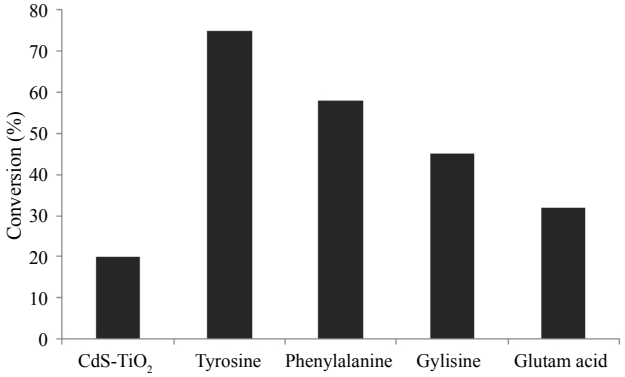

Fig. 9. The effect of opted amino acid for surface modification on the NB conversion (%) (catalyst: 0.1 g, NB: 0.0136 M, irradiation time: 120 min, pH: netural).

we can find out that the conversion of modified CdS-TiO_2 was higher than that of bared CdS-TiO_2, while the photoconversion efficiency decreased according to the following: Tyrosine-CdS-TiO_2>Phenylalanine-CdS-TiO_2>Glaysine-CdS-TiO_2>Glutamate/CdS-TiO_2. Obviously, Tyrosine-CdS-/TiO_2 is the most active catalyst in aqueous condition. The results indicate that the reaction is influenced by the surface of TiO_2. In addition, coupling of CdS with TiO_2 can delay the electron hole recombination in titanium dioxide (which is active in the UV region). Different amino acids were taken in to modify CdS-TiO_2 for the positive effect on conversion of NB to Aniline. The loading of amino acids increased both the adsorption of NB and photocatalyst activity. Adding the amino acids can prevent the electron hole recombination, because they have strong electron donating properties and act as a hole trap. In addition, amino acids ameliorate the coupling between NB and CdS-TiO_2, and transferring electrons from the conduction band of CdS-TiO_2 to NB can be conducted with negligible activation energy [3]. The photoactivity yield is highest for the modified photocatalyst with tyrosine due to the presence of the phenyl group in the tyrosine structure which is similar to the NB structure. Therefore, the adsorption of NB increases compared to glysine, phenylalanine and glutamate. In addition, the OH group on the tyrosine structure participates in both hydrogen bonding and π-π interaction between the amino acid and support. This results in an increase in the photocatalytic conversion yield.

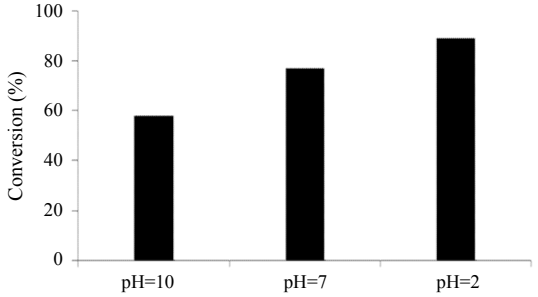

Fig. 10. The effect of acidic, natural and basic media on the conversion of NB (%) (catalyst: 0.1 g, NB: 0.0136 M, irradiation time: 120 min)

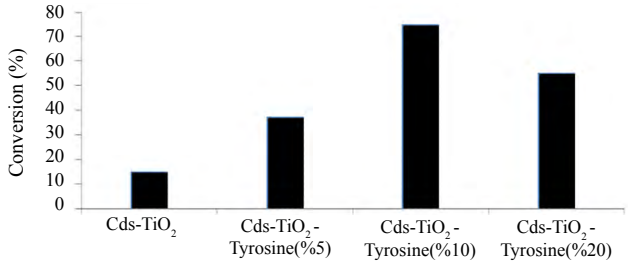

Fig. 11. The effect of amount of loaded amino acid on the conversion (%) of NB (catalyst: 0.1 g, NB: 0.0136 M, irradiation time: 120 min, pH: neutral)

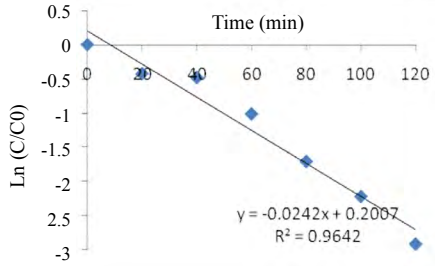

Fig. 12. Kinetic study of NB photoreduction (catalyst: 0.1 g, NB: 0.0136 M, under optimized conditions)

The effect of pH

The effect of pH on the photoactivity of Tyrosine-CdS-TiO_2 has been studied and the results are shown in Fig. 10. From Fig. 10 we can find out that by increasing the acidity of the medium, the photocatalytic efficiency enhances. This can be related to the structural reformation of the photocatalyst surface. Fig. 3 shows the FTIR analysis for these composites after being used in acidic and basic conditions. The appearance of new peaks at 825, 1245 cm^{-1} in the acidic medium is related to the amino benzene stretching vibration in the photocatalytst. This observation shows that during the photoreduction conversion of nitrobenzene, a part of products (such as aniline) is strongly bonded to the photocatalyst after being formed. Thus, the photoctalyst surface is being rich of electron donating agents (both amino acid and aniline), the electron hole recombination delays and the efficiency enhances.

The effect of loaded amino acid

The effect of amino acid loading on photoredudtion of NB was studied in the range of 5% to 20% of amino acid and the results were compared with pure CdS-TiO_2 presented in Fig. 11. Photoactivity can be related to the availability of active sites on the TiO_2 surface. Increasing the tyrosine amount enhances the photoconversion rate. Tyrosine can enhance the efficiency by trapping the holes from the CdS-TiO_2 photoactivity and reducing the electron-hole recombination. The photoreduction efficiency is enhanced up to 10% of the amount of amino acid, but then decreases due to the covering of active sites of CdS-TiO_2 surface and light scattering. Therefore, we used 10% loaded amino acid as the optimum amount during the next experiments.

Kinetic study

Fig. 12 shows the kinetics of NB (solubility 0.2g/100 ml in water) photoreduction for an initial concentration of 0.0136 M under the optimized conditions with CdS-TiO_2-Tyrosine. The results indicated that the photocatalytic reduction of the NB can be described by the first-order kinetic model, $\ln(C_0/C) = kKt = k_{app}t$.

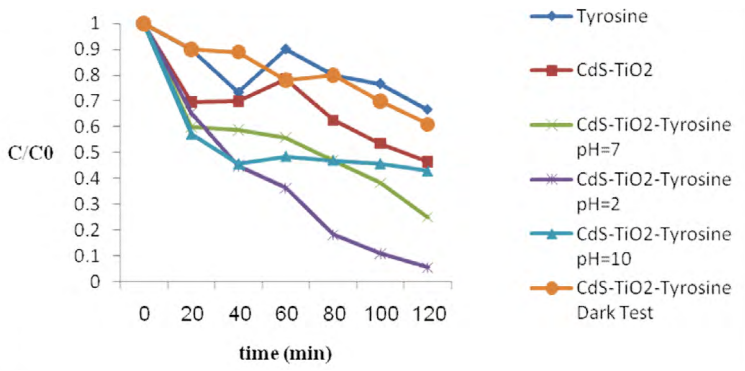

Fig. 13. The results of NB photoreduction with different catalysts and conditions (catalyst: 0.1 g, NB: 0.0136 M)

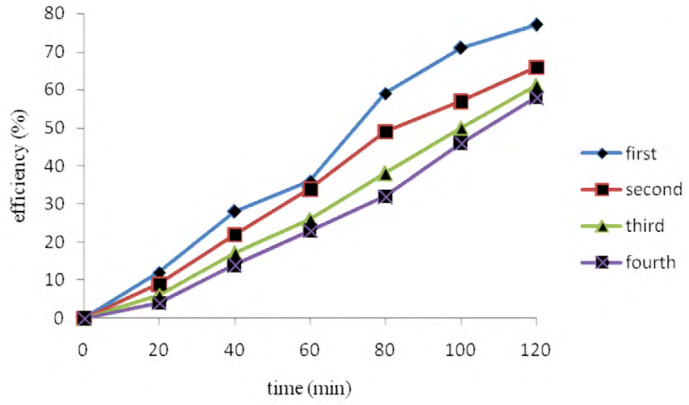

Fig. 14. Reused experiments of Tyrosine-CdS-TiO2 irradiated by visible light (catalyst: 0.1 g, NB: 0.0136 M, pH: neutral)

The semi logarithmic plots of the concentration data give a straight line. The correlation constant for the fitted line was calculated to be R^2= 0.96 for acidic media, 0.1 g photocatalyst and 10% coated amino acid as the optimized conditions. The rate constant for conversion of NB was calculated to be 0.024 min^{-1}. This constant is a function of many operational conditions. The results of photoreduction of NB with a different type of catalysts and operational conditions are presented in Fig. 13. It is clear that the maximum photoconversion takes place in the case of CdS-TiO_2-Tyrosine in acidic media whereas the minimum one takes place in the case of Tyrosine after 2 h.

Reusability tests

Tyrosine-CdS-TiO_2 was reused as the best photocatalyst for four times and the retrieval efficiency for NB photoreduction was above 58%. Fig. 14 shows the experimental results. (1), (2), (3) and (4) represent the first, second, third and fourth time of repeated use, respectively. To follow this parameter, after each test, the dispersed photocatalytic particles were collected from the reaction media by centrifuging and filtering the suspension. The solid washed with water and ethanol three times, dried at 60 °C overnight, and crushed to fine powder for further using.

CONCLUSIONS

The effect of the amino acids for surface modification of CdS-TiO_2 photocalaysts and their activities toward the NB photoconversion were investigated. The results indicated that the highest photoconversion efficiency and adsorption are achieved with tyrosine. Tyrosine with a phenol ring has a compatible structure with NB. Therefore, the absorption capability and photoconversion noticeably increased when we used CdS-TiO_2-Tyrosine compared to the others. The study also included studying the effect of pH showing that by increasing the acidity of the medium, the photoconversion efficiency is also increased. The FT-IR spectra showed peaks at 825 and 1245 cm^{-1} in the acidic medium related to the bonded aniline to CdS-TiO_2-Tyrosine surface which enhanced the photocatalytic efficiency acting as an electron-donating agent. This study proposes a promising modified photocatalyst based on CdS-TiO_2 for photoconversion of wastewaters containing nitroaromatic compounds.

CONFLICT OF INTERESTS

The authors declare that there is no conflict of interests regarding the publication of this paper.

REFERENCES

1. Padervand M, Salari H, Ahmadvand S, Gholami MR. Removal of an organic pollutant from waste water by photocatalytic behavior of AgX/TiO2 loaded on mordenite nanocrystals. Research on Chemical Intermediates. 2012;38(8):1975-85.
2. Qin Q, Ma J, Liu K. Adsorption of nitrobenzene from aqueous solution by MCM-41. Journal of Colloid and Interface Science. 2007;315(1):80-6.
3. Koh M, Nakajima T. Adsorption of aromatic compounds on CxN-coated activated carbon. Carbon. 2000;38(14):1947-54.
4. Yang Y, Ma J, Qin Q, Zhai X. Degradation of nitrobenzene by nano-TiO2 catalyzed ozonation. Journal of Molecular Catalysis A: Chemical. 2007;267(1):41-8.
5. Nishino SF, Spain JC. Oxidative Pathway for the Biodegradation of Nitrobenzene by Comamonas sp. Strain JS765. Applied and environmental microbiology. 1995;61(6):2308-13.
6. Nishino SF, Spain J. Degradation of nitrobenzene by a Pseudomonas pseudoalcaligenes. Applied and environmental microbiology. 1993;59(8):2520-5.
7. Padervand M. Ionic liquid mediated synthesis of AgBr–Ag3PO4 nanostructures as highly efficient visible-light photocatalysts. Materials Research Innovations. 2016:1-7.
8. Taghavi Fardood S, Ramazani A, Golfar Z, Joo SW. Green synthesis of Ni-Cu-Zn ferrite nanoparticles using tragacanth gum and their use as an efficient catalyst for the synthesis of polyhydroquinoline derivatives. Applied Organometallic Chemistry. 2017:e3823-n/a.
9. Sadri F, Ramazani A, Ahankar H, Taghavi Fardood S, Azimzadeh Asiabi P, Khoobi M, et al. Aqueous-phase oxidation of alcohols with green oxidants (Oxone and hydrogen peroxide) in the presence of MgFe2O4 magnetic nanoparticles as an efficient and reusable catalyst. Journal of Nanostructures. 2016;6(4):264-72.
10. Arabian R, Ramazani A, Mohtat B, Azizkhani V, Joo SW, Rouhani M. A Convenient and Efficient Protocol for the Synthesis of HBIW Catalyzed by Silica Nanoparticles under Ultrasound Irradiation. Journal of Energetic Materials. 2014;32(4):300-5.
11. Fardood ST, Atrak K, Ramazani A. Green synthesis using tragacanth gum and characterization of Ni–Cu–Zn ferrite nanoparticles as a magnetically separable photocatalyst for organic dyes degradation from aqueous solution under visible light. Journal of Materials Science: Materials in Electronics. 2017;28(14):10739-46.
12. Taghavi Fardood S, Ramazani A, Moradi S, Azimzadeh Asiabi P. Green synthesis of zinc oxide nanoparticles using arabic gum and photocatalytic degradation of direct blue 129 dye under visible light. Journal of Materials Science: Materials in Electronics. 2017.
13. Padervand M. Facile Synthesis of the Novel Ag[1-butyl 3-methyl imidazolium]Br Nanospheres for Efficient Photodisinfection of Wastewaters. Chemical Engineering Communications. 2016;203(11):1532-7.
14. Billotey C, Wilhelm C, Devaud M, Bacri JC, Bittoun J, Gazeau F. Cell internalization of anionic maghemite nanoparticles: Quantitative effect on magnetic resonance

imaging. Magnetic Resonance in Medicine. 2003;49(4):646-54.

15. Padervand M. Visible-light photoactive Ag-AgBr/[alpha]-Ag^ sub 3^ VO^ sub 4^ nanostructures prepared in a water-soluble ionic liquid for degradation of wastewater. Applied Nanoscience. 2016;6(8):1119.
16. Padervand M, Karanji AK, Elahifard MR. Copper, gold, and silver decorated magnetic core–polymeric shell nanostructures for destruction of pathogenic bacteria. Russian Journal of Physical Chemistry A. 2017;91(5):936-45.
17. Li Q, Li X, Wageh S, Al-Ghamdi AA, Yu J. CdS/Graphene Nanocomposite Photocatalysts. Advanced Energy Materials. 2015;5(14):1500010-n/a.
18. Li G-S, Zhang D-Q, Yu JC. A New Visible-Light Photocatalyst: CdS Quantum Dots Embedded Mesoporous TiO2. Environmental Science & Technology. 2009;43(18):7079-85.
19. Padervand M, Tasviri M, Gholami M. Effective photocatalytic degradation of an azo dye over nanosized Ag/AgBr-modified TiO2 loaded on zeolite. Chemical Papers2011. p. 280.
20. Elahifard M, Padervand M, Yasini S, Fazeli E. The effect of double impurity cluster of Ni and Co in TiO2 bulk; a DFT study. Journal of Electroceramics. 2016;37(1):79-84.
21. Padervand M, Reza Elahifard M, Vatan Meidanshahi R, Ghasemi S, Haghighi S, Reza Gholami M. Investigation of the antibacterial and photocatalytic properties of the zeolitic nanosized AgBr/TiO2 composites. Materials Science in Semiconductor Processing. 2012;15(1):73-9.
22. Mele G, Garcìa-Lòpez E, Palmisano L, Dyrda G, Słota R. Photocatalytic Degradation of 4-Nitrophenol in Aqueous Suspension by Using Polycrystalline TiO2 Impregnated with Lanthanide Double-Decker Phthalocyanine Complexes. The Journal of Physical Chemistry C. 2007;111(17):6581-8.
23. Ramazani A, Hamidi S, Morsali A. A novel mixed-ligands holodirected two-dimensional lead(II) coordination polymer as precursor for preparation lead(II) oxide nanoparticles. Journal of Molecular Liquids. 2010;157(1):73-7.
24. Wu L, Yu JC, Fu X. Characterization and photocatalytic mechanism of nanosized CdS coupled TiO2 nanocrystals under visible light irradiation. Journal of Molecular Catalysis A: Chemical. 2006;244(1):25-32.
25. Qian S, Wang C, Liu W, Zhu Y, Yao W, Lu X. An enhanced CdS/TiO2 photocatalyst with high stability and activity: Effect of mesoporous substrate and bifunctional linking molecule. Journal of Materials Chemistry. 2011;21(13):4945-52.
26. Huang H, Zhou J, Liu H, Zhou Y, Feng Y. Selective photoreduction of nitrobenzene to aniline on TiO2 nanoparticles modified with amino acid. Journal of Hazardous Materials. 2010;178(1):994-8.
27. Fardood ST, Ramazani A, Moradi S. Green synthesis of Ni–Cu–Mg ferrite nanoparticles using tragacanth gum and their use as an efficient catalyst for the synthesis of polyhydroquinoline derivatives. Journal of Sol-Gel Science and Technology. 2017;82(2):432-9.